EPSC Abstracts
Vol. 12, EPSC2018-841, 2018
European Planetary Science Congress 2018

Ceres' surface observed at low phase angles by VIR-Dawn

M. Ciarniello (1), M. C. De Sanctis (1), E. Ammannito (2), A. Raponi (1), F. G. Carrozzo (1), A. Longobardo (1,3), F. Tosi (1), E. Rognini (1), F. Zambon (1), S. Schroeder (4), C. A. Raymond (5), C. T. Russell (6) and the VIR team.
(1) IAPS-INAF, Rome, Italy, (2) ASI, Rome, Italy, (3) DIST, Università Partenope, Naples, Italy, (4) DLR, Berlin, Germany, (5) Jet Propulsion Laboratory, California Institute of Technology, Pasadena, CA, USA, (6) University of California Los Angeles, Earth Planetary and Space Sciences, Los Angeles, CA, USA; (mauro.ciarniello@iaps.inaf.it)

Abstract

We take advantage of low phase angle observations performed by the VIR-Dawn spectrometer to extend the investigation of Ceres' surface phase curve in the opposition effect regime. The Hapke's spectrophotometric model and Monte Carlo simulations are compared to VIR data to infer physical properties of the regolith covering Ceres' surface.

1. Introduction

The opposition effect (OE) is a surge of reflectance commonly detected on the surface of atmosphereless bodies [1,2,3], when observed at low phase angles.
The acquisitions obtained by the Visible and InfraRed mapping spectrometer (VIR [4], 0.25-5.1 μm spectral interval) on-board the Dawn mission, during the Extended Mapping Orbit 4 (XMO4) mission phase, allowed the observation of Ceres' surface down to ~0° phase angle, permitting the characterization of the OE. This set of measurements complements previous observations performed during Dawn mission at Ceres, that covered the 7°-132° phase angle range, and allows to extend the analysis of the Ceres's spectrophotometric properties reported in [5].
Here we report about preliminary results from the analysis of these new set of observations, by means of Hapke's photometric model [1] and Monte Carlo ray-tracing [6].

2. Hapke's model and Ceres's phase curve

In [2] Ceres' spectrophotometric properties have been investigated by means of a simplified Hapke's model following the formulation reported in the equation below:

$$\frac{I}{F} = \frac{w}{4}\frac{\mu_{0eff}}{\mu_{0eff}+\mu_{eff}}\left[\left(1+B(\alpha)\right)p(\alpha) + H\left(w,\mu_{0eff}\right)H\left(w,\mu_{eff}\right) - 1\right]S(i,e,\alpha,\bar{\theta}) \quad (1)$$

with
I/F: radiance factor; *w:* single scattering albedo; *α,i,e:* phase, incidence and emission angles, respectively; *p(α):* single particle phase function (SPPF) modeled with a two-parameter Henyey-Greenstein formulation [1]; *B(α):* Shadow hiding OE function depending on OE amplitude (B_0) and angular width (h); $S(i,e,\alpha,\bar{\theta})$: large scale roughness shadowing function, depending on the average surface roughness slope $\bar{\theta}$; *H(w,x):* Chandrasekhar function; μ_{0eff}, μ_{eff}: cosine of the effective incidence and emission angle, respectively.
Assuming Eq. 1, this can be rearranged as follows:

$$\frac{I/F}{D} = \frac{w}{8}\left[\left(1+B(\alpha)\right)p(\alpha) + H\left(w,\mu_{0eff}\right)H\left(w,\mu_{eff}\right) - 1\right] \quad (2)$$

with $D = \frac{2\mu_{0eff}}{\mu_{0eff}+\mu_{eff}}S(i,e,\alpha,\bar{\theta})$.

We refer to the quantity $\frac{I/F}{D}$ reported in Eq. 2 as Ceres' "phase function" since it is mostly dependent on phase angle, while, given the low albedo of Ceres' surface, dependence on incidence and emission angle through the *H* functions is small.

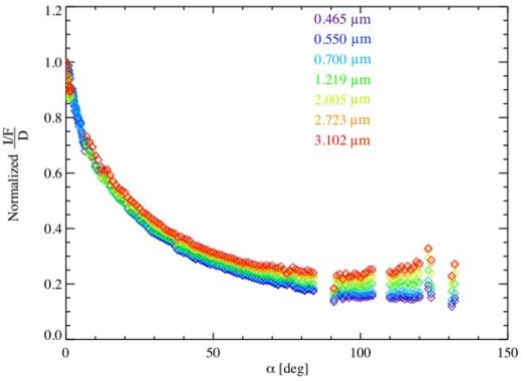

Figure 1. Ceres' phase function at different wavelengths.

In Fig. 1, Ceres' phase function as derived from VIR observations at different wavelengths is shown after normalization at 0°. The curve has been computed by averaging in 0.2° phase angle bins observations from the XMO4 phase for α<7°, while for α>7° the Ceres Approach (CSA), Rotational Characterization 3 (RC3), Ceres Transfer to Survey (CTS), and Ceres Survey (CSS) sequences have been considered (averaged in 1° bins). It can be noted that Ceres' phase function is progressively more forward-scattering for increasing wavelengths.

3. Opposition Effect on Ceres

OE in particulate media is typically attributed to two different mechanisms [1 and references therein]: Shadow Hiding Opposition Effect (SHOE) and Coherent Backscattering Opposition Effect (CBOE). SHOE is produced by a progressive reduction of the visibility of the shadows cast by particles in the top layers of the surface on the ones below, for decreasing phase angles, while CBOE is the effect of the constructive interference at low phase angles between waves propagating in the medium along the same path but in opposite directions. The angular width of SHOE is typically of the order of ~10°-20°, and is considered not to depend on wavelength [1], being mainly driven by light scattered once in the medium. Conversely, CBOE angular width, is typically smaller than SHOE (~1°-2°, [1,2]), and may show wavelength dependence.

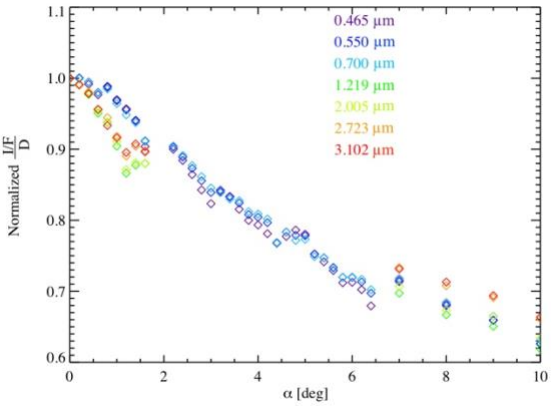

Figure 2. Ceres' phase function, in the 0°-10° phase angle range, at different wavelengths.

In Fig. 2, Ceres' phase curve at small phase angles (α<10°) is shown at different wavelengths. It can be noted that there is no clear spectral dependence of the OE angular width. The observed variability for α<2°, which could be indicative of a contribution from CBOE, in particular at IR wavelengths, is most likely related to the fact that different phase angles sample different regions of the surface, because of the poor observations redundancy. Moreover, the reflectance surge for decreasing α does not show strong evidence of an additional contribution at the smallest phase angles, which could be indicative of CBOE superimposed on the wider SHOE. Although an unambiguous assessment of CBOE requires polarimetry measurements [3], the arguments provided above suggest that SH is the principal mechanism causing OE on Ceres.

4. Hapke's model parameters

XMO4 observations permits to extend the phase angle range investigated in [5] by characterizing the OE region of Ceres' surface phase function, and allow us to derive improved sets of Hapke's model parameters, across the whole VIR spectral range. This is done by fitting the phase function to Eq. 2, and various solutions have been studied, depending on different a priori assumptions on Hapke's model parameters. For example, assuming that B_0 cannot exceed 1, as required from SHOE physics, and $\bar{\theta}$=29° from [5], we derive a preliminary solution at 0.55 µm with $B_0=1$, $h=0.037$, $b=0.40$ $c=0.23$, $w=0.15$. Such a value of w is representative of a low albedo surface, while b and c are compatible with particles characterized by an intermediate level of internal scatterers, according to [7]. Finally, the SHOE angular width (h) can be related to the porosity (P) of the regolith (Eq. 9.26 in [1]) and the derived value corresponds to P=0.91, indicating a highly porous material.

5. Monte Carlo simulations

At the scope to further characterize the porosity of the surface, we perform a preliminary comparison of Ceres' reflectance curve with the output of Monte Carlo (MC) ray-tracing simulations [6]. MC simulations performed for different filling factors of the modeled regolith in the range Φ=0.01-0.3, indicate, as expected, that smaller porosities provide larger SHOE widths, and Ceres' reflectance curve is better matched by MC simulations with Φ between 0.05-0.1, (P=0.9-0.95). This is compatible with the result derived from the Hapke's model.

Acknowledgements

This work is supported by the Italian Space Agency (ASI, ASI-INAF n. I/004/12/1) and NASA. Enabling contributions from the Dawn Instrument, Operations, and Science Teams are gratefully acknowledged.

References

[1] Hapke B.W. (2012), Theory of reflectance and emittance spectroscopy. [2] M. Mishchenko (1992), Astrophys. Space Sci. 194, 327–333. [3] Nelson et al. (2000), Icarus, 147, 545–558. [4] De Sanctis, M. C. et al. (2011), Space Sci. Rev., 163, 329. [5] Ciarniello, M. et al. (2017), A&A 598, A130. [6] Ciarniello et al., (2014). Icarus 237, 293–305. [7] McGuire A. F. and Hapke B. W. (1995), Icarus 113, 134-155.